UNCECOMP 2017
2nd ECCOMAS Thematic Conference on
Uncertainty Quantification in Computational Sciences and Engineering
M. Papadrakakis, V. Papadopoulos, G. Stefanou (eds.)
Rhodes Island, Greece, 15–17 June 2017

AERODYNAMIC SHAPE OPTIMIZATION UNDER FLOW UNCERTAINTIES USING NON-INTRUSIVE POLYNOMIAL CHAOS AND EVOLUTIONARY ALGORITHMS

Athanasios G. Liatsikouras[1,2*], Varvara G. Asouti[1], Kyriakos C. Giannakoglou[1], Guillaume Pierrot[3], Mustafa Megahed[2]

[1]National Technical University of Athens
School of Mech. Eng., Parallel CFD & Optimization Unit, Athens, Greece
{liatsi,kgianna}@central.ntua.gr, vasouti@mail.ntua.gr

[2] ESI Software Germany GmbH
Kruppstr. 90, ETEC H4, 3.OG, 45145, Essen, Germany
{athanasios.liatsikouras, mustafa.megahed}@esi-group.com

[3] ESI - Group
99 Rue des Solets, 94513 Rungis, France
guillaume.pierrot@esi-group.com

Keywords: Optimization under Uncertainties, Shape Optimization, Non-Intrusive Polynomial Chaos, Radial Basis Functions, Harmonic Coordinates, Shape Smoothing, Mesh Morphing.

Abstract. *The existence of uncertainties, associated with the operating conditions or manufacturing imperfections, occur quite often in aerodynamic optimization problems. In this paper, a workflow for shape optimization in the presence of environmental uncertain flow conditions, varying stochastically around an average value with an a–priori known standard deviation, is presented. To do so, the Uncertainty Quantification (UQ) for the objective function needs to be carried out. This is based on the non-intrusive Polynomial Chaos Expansion (niPCE) method [1], which allows for a controllable number of calls to the CFD tool used to evaluate each candidate solution, compared to other sampling methods such as Monte–Carlo. Within the proposed workflow, PCE is combined with the optimization platform EASY (Evolutionary Algorithms SYstem) [2], which undertakes the optimization task. The overall process is fully automated. The shape under consideration is parameterized using CAD-free approaches, such as Radial Basis Function techniques or the combined use of two cages and the corresponding Harmonic Coordinates, which are responsible only for surface deformations whereas, as it will be explained below, other morphing/smoothing [3] tool undertakes the adaptation of the CFD mesh to the updated boundaries at each optimization cycle. The PCE method selects the points (Gaussian nodes) in the design space to be evaluated and the computed performance metrics are integrated with weights indicated by the Gauss integration rules, in order to compute the mean value and standard deviation of the objective function of the flow problem under uncertainties. The aforementioned tools are applied in two problems, in which OpenFOAM is the CFD evaluation software.*

1 INTRODUCTION

In aerodynamics, shape optimization under uncertainties [4, 5] aims at designing a shape that performs efficiently in a range of operating points determined by stochastically varying flow conditions or in the presence of manufacturing imperfections. In this paper, a workflow that performs 2D or 3D aerodynamic shape optimizations under uncertainties, exclusively caused by variations in the flow conditions, is presented and demonstrated in two cases.

Let us denote the function characterizing the performance of an aerodynamic body (at a single operating point) by $F{=}F(\vec{b},\vec{U}(\vec{b}))$, where $\vec{b}{\in}\mathbb{R}^N$ is the design vector controlling the shape and $\vec{U}$ denotes the flow variables. In the presence of uncertain flow conditions, the objective function to be optimized can be generally expressed as $\hat{F}{=}\hat{F}(\vec{c},F(\vec{c},\vec{b},\vec{U}(\vec{b},\vec{c})))$ to denote the dependency of $\hat{F}$ on the stochastically varying environmental variables $\vec{c}\in\mathbb{R}^M$. One of the most frequently used forms of $\hat{F}$ is

$$\hat{F}=\hat{\mu}_F \pm \kappa\hat{\sigma}_F \tag{1}$$

in which $\hat{F}$ is expressed as a linear combination of the mean value ($\hat{\mu}_F$) of F and its standard deviation ($\hat{\sigma}_F$) weighted by κ. In the literature, there are some, stochastic or deterministic, methods of computing/estimating the mean value and the standard deviation of a function. A well-known stochastic technique is the Monte–Carlo (MC) [6] one, which may become very expensive in terms of CPU, since a great number of stochastic variable data-sets should be evaluated by the CFD software (in CFD-based shape optimization problems). To decrease the cost of MC, techniques such as Quasi-MC [7] and Latin-Hypercube Sampling [8] have been developed. On the other hand, a rival method to cope with the same problem is the Method of Moments [9], in which the adjoint method [10] and direct differentiation are used to compute up to second–order derivatives of F with respect to (w.r.t.) the environmental variables $\vec{c}$ in order to get the first two statistical moments of F with second-order accuracy. This method proves to be a viable alternative of MC techniques, though its computational cost depends on the number of stochastic variables. In case of a gradient-based optimization method, $\hat{F}$ needs to be differentiated w.r.t. the design variables $\vec{b}$, which means that third–order mixed derivatives of F w.r.t the environmental (twice) and the design variables (once) are required. This has been presented, for the first time in the literature, by the NTUA group in [9, 11].

In this work, the computation of the $\hat{\mu}_F$ and $\hat{\sigma}_F$ relies on the PCE technique [1, 12]. There are two ways to implement this technique, the intrusive and non-intrusive one. In the intrusive PCE variant, every uncertainty affecting the flow model should be introduced in the governing equations, adding complexity to the problem to be solved. In the non-intrusive variant, which is the one used herein, the evaluation software is used as black–box to compute the objective function values for predefined data–sets of the uncertain variables. The latter are the Gaussian nodes determined by the Gauss integration rules according to which the computation of $\hat{\mu}_F$ and its $\hat{\sigma}_F$ is the weighted sum of F taken on at these nodes.

2 THE PROPOSED WORKFLOW AND ITS CONSTITUENTS

In shape optimization, a technique to parameterize the aerodynamic shapes should be available. In this framework, CAD–free approaches using either Radial Basis Functions (RBF) or control cages based on the Harmonic Coordinates (HC) are employed. The coordinates of the RBF centers or the HC cage knots form the design variables vector ($\vec{b}$). Over and above, a mesh morpher/smoother (Rigid Motion Mesh Morpher; R3M) is used to adapt the deformations in the 3D computational mesh. The latter is generated for the reference geometry using CFD–GEOM

[13]. Regarding the uncertain variables (flow conditions), it is assumed that these follow a normal distribution around an a–priori known average value and standard deviation. The general purpose optimization platform EASY (Evolutionary Algorithms SYstem, [2]) undertakes the optimization through Metamodel–Assisted Evolutionary Algorithms, MAEAs [14, 15]. The overall workflow is outlined in Fig. 1.

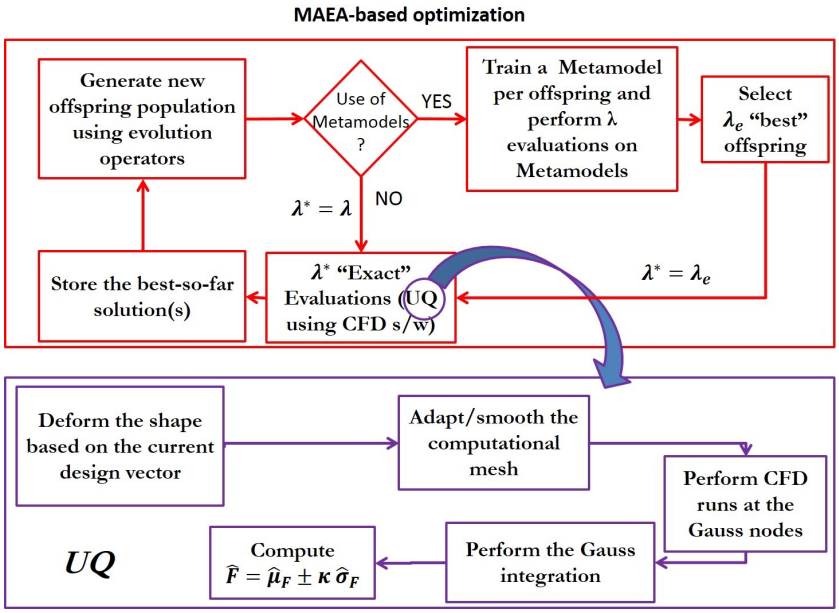

Figure 1: Workflow for CFD-based shape optimization under uncertainties.

2.1 Optimization Platform

The EASY software [2] can handle single- or multi-objective, constrained or unconstrained, optimization problems by accommodating any evaluation software as a black–box. EASY implements a population–based Evolutionary Algorithm (EA) that handles three populations, namely the parents, offspring and elites and applies evolution operators in conformity with the binary or real encoding of the design variables. For each offspring, the UQ w.r.t. a performance metric F (such as the drag, lift, losses, etc.) should be carried out. This is based on the niPCE where the evaluation tool (herein the CFD s/w) is used, for different sets of the uncertain variables, along with the Gauss quadrature integration formula. Among the important features of EASY is the smart use of low–cost surrogate evaluation models (metamodels; artificial neural networks) during the optimization giving rise to the so-called Metamodel–Assisted EA (MAEA). This is appropriate for computationally demanding problems such as those with uncertainties, where the niPCE requires many calls to the CFD tool. In the MAEA, local metamodels, on–line trained for each and every new individual generated during the evolution, are used. For all but the first few generations, the metamodels are used to pre–evaluate the offspring population by, practically, interpolating the $\hat{F}$ value using archived previously evaluated individuals and only the most promising members (according to the pre–evaluation on metamodels) are selected to undergo CFD–based evaluation.

2.2 Control of the Shape and Mesh Morphing

This section describes briefly the two CAD–free approaches utilized in this workflow, based either on RBF networks or HC cages. These tools are responsible only for modifying the shapes whereas the CFD mesh is adapted to the changed shape using a mesh morpher.

2.2.1 Radial Basis Function Model

The use of the RBF model involves two steps, namely training and implementation. Initially, the user has to define the so–called RBF centers. The K RBF centers can either be a subset of the mesh nodes lying on the shape to be optimized or some user–defined nodes around it. The coordinates of the RBF centers form the design vector. The displacement $\Delta\vec{r}$ of any CFD node on the shape, initially located at $\vec{r}$, is given by

$$\Delta\vec{r} = \sum_{i=1}^{K} \vec{w}_i \phi(||\vec{r}_{ci} - \vec{r}||) \tag{2}$$

where $\vec{r_{ci}}$ is the initial position vector of the RBF center i, ϕ is the RBF activation function and $\vec{w}_i$ weight coefficients, as many as the RBF centers, for each Cartesian direction. To compute them, the model needs to be trained and, to this end, eq.2 is applied K times on the K centers of the RBF model and needs to be satisfied for all Cartesian coordinates. For the training, the displacements $\Delta\vec{r}$, of the RBF centers, generated anew during the evolution, are used.

2.2.2 The Harmonic Coordinates two–cage Model

Cages based on HC, initially proposed for character articulation [16] is a technique to parameterize the points in a 2D or 3D domain. In an HC–cage–based parameterization, surface deformations are controlled by the so–called "cage" (a topologically flexible structure) that encloses the surface under consideration. An HC–based technique that may control both shape deformations and CFD mesh adaptation (not used, though, in the problems studied in this paper) to the new geometry has been proposed in [17], by adopting a two–cage control mechanism. The cages are filled with a quite coarse unstructured mesh and the nodal HC values on the coarse mesh are computed by solving as many Laplace equations as the cage control vertices, with appropriate boundary conditions. The HC fields are, then, interpolated from the cage nodes to the CFD mesh nodes. Thus, the CFD mesh (or its boundary only, as in the examined problems) can be controlled by displacing the HC cage control vertices, which become the design variables in the optimization problem. In the two-cage structure, the inner cage controls both the shape deformation and mesh morphing while the outer cage limits the effect of morphing and guarantees a smooth transition, without inverted elements, between the CFD mesh parts that lie inside and outside the outer cage. Thus, the outer cage vertices should remain still during the optimization and Laplace equations are not solved for them.

2.2.3 Morphing–Smoothing Tool

Usually, whenever a CAD–free parameterization tool, such as HC cages or RBF networks, is used, the same tool can also undertake the adaptation/deformation of the CFD mesh to the updated shapes. However, in the workflow presented herein, the CFD mesh adaptation is controlled by a mesh morpher.

In the literature, several morphing techniques such as those in may be found. Most of them cannot handle mesh anisotropies. The Rigid Motion Mesh Morpher and its adaptive smoother (R3M) [3], used in this work, is a meshless method and belongs to the optimization–based methods. The internal nodes of the CFD mesh are displaced so as to minimize a given distortion metric. Therefore, it can handle mesh anisotropies since it favours rigidity in the critical directions of imminent distortion. The basic idea is to keep some parts/elements of the CFD mesh (referred to as stencils) as-rigid-as-possible. An example of such a stencil handled by the morpher could be a cluster of neighbouring grid nodes. By definition, 'Rigid Motion' refers to a movement of a body without changing its shape or size. Obviously, this cannot be kept entirely rigid, since this would be in contrast with the mesh adaptation, even if there are ways to favour rigidity in the critical directions, when distortion of an element/part becomes imminent.

If a stencil (s) in motion was totally rigid, its motion could be associated with a translation and a rotation velocity, $\vec{\alpha}_s$ and $\vec{b}_s$ respectively. In this case, the velocity of any node i belonging to this stencil would be

$$u_{is} = \vec{\alpha}_s + \vec{b}_s \times (\vec{x}_i - \vec{c}_s) \tag{3}$$

where $\vec{x}_i$ is the position vector of node i that belongs to stencil s. Since the motion of a stencil cannot always be entirely rigid, the actual velocity of node i would be $u_i \neq u_{is}$. R3M and its smoother tends to minimize the difference between these two velocities (with some weighting coefficients w_s and μ_{js}) for each and every stencil node. Moreover, in order to enforce smoothness of the surface, a subset of its nodes are selected as handles which control surface changes. For each handle node, there is also an underlying node which is free to move with a different velocity. By displacing the handle nodes (Fig. 2), the CFD mesh nodes are moved by minimizing the so–called 'Morpher's Energy'

$$E = \sum_s w_s \sum_{j \in s} \mu_{js} \left[\vec{u}_j - \vec{\alpha}_s - \vec{b}_s \times (\vec{x}_j - \vec{c}_s) \right]^2 + \sum_{i \in H} \lambda_i \left(\vec{u}_i - \vec{V}_i^t \right)^2 \tag{4}$$

where $\vec{u}_j$ is the actual velocity of node j, $\vec{x}_j$ is its position vector, c_s the center of the gravity of the stencil s, $\vec{V}_i^t$ is the so–called target velocity of the handle (displacement of CFD mesh node i on the shape) and λ_i a weighting coefficient standing for the stiffness of a spring connecting the handle with its underlying node. If N_n is the number of all the CFD mesh nodes (including the surface nodes), N_s the number of stencils and N_h the number of handles, then the unknowns in eq. 4 are the N_n nodal velocities ($\vec{u}_i$), the N_s translation velocities ($\vec{\alpha}_s$) and the N_s rotation velocities ($\vec{b}_s$) of the stencils. Once the N_h target velocities of the handles become known, the morpher's energy, eq. 4, is minimized in the least squares sense, by finding the stationary points w.r.t. the corresponding unknowns by satisfying $\frac{\partial E}{\partial \vec{u}_j}$=0, $\frac{\partial E}{\partial \vec{\alpha}_s}$=0 and $\frac{\partial E}{\partial \vec{b}_s}$=0, [3].

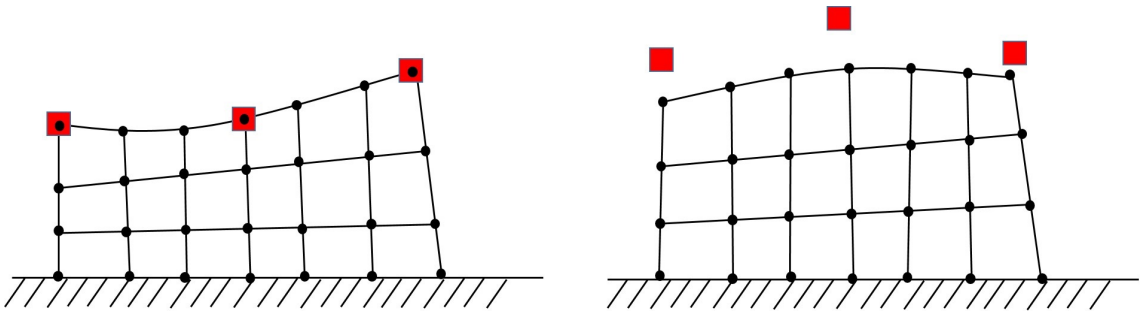

Figure 2: For any displacement of the handles (red squares) $\vec{V}_i^t$, the minimization of the energy expressed in eq. 4 computes the displacements of the CFD nodes.

2.3 UQ using Non-Intrusive PCE

Let $F(\vec{\xi})$ be a stochastic function, where $\vec{\xi}$ is stochastic variable and $w(\vec{\xi})$ its probability density function (PDF). We also assume a family of orthogonal polynomials $\Psi_i(\vec{\xi})$, where i is the maximum degree of each polynomial. According to the PCE theory [1], F can be approximated through the linear combination of orthogonal polynomials $\Psi_i(\vec{\xi})$,

$$F(\vec{\xi}) \simeq f(\vec{\xi}) = \sum_{i=0}^{q} \alpha_i \Psi_i(\vec{\xi}) \tag{5}$$

where q is the user-defined chaos order, truncating eq. 5 which might otherwise have an infinite number of terms. The mean value (μ_F) and variance (σ_F^2) of F can be expressed as

$$\hat{\mu}_F = \int f(\vec{\xi}) w(\vec{\xi}) d\vec{\xi} \ , \ \hat{\sigma}_F^2 = \int \Big(f(\vec{\xi}) - \hat{\mu}_F \Big)^2 w(\vec{\xi}) d\vec{\xi} \tag{6}$$

By developing eqs. 6 and making use of appropriate Galerkin projections, the final expressions of the first two statistical moments of F, become

$$\hat{\mu}_F = \alpha_0 \ , \ \hat{\sigma}_F = \sqrt{\sum_{i=1}^{q} \alpha_i^2} \tag{7}$$

The PCE coefficients required in eqs. 7 result from the following integrals

$$\alpha_i = \int_D F(\vec{\xi}) \Psi_i(\vec{\xi}) w(\vec{\xi}) d\vec{\xi}, \qquad i = 0, 1, \ldots, q \tag{8}$$

where D is the design space in which F is defined.

The integrals in eq. 8 can be evaluated by the Gauss quadrature integration formula in the domain D. According to this, each integral can be approximated by the weighted sum of the performance metric F values at n (the value of n depends on the desired accuracy) points z_i within the domain of integration, namely

$$\int_D F(\vec{\xi}) w(\vec{\xi}) d\vec{\xi} = \sum_{i=1}^{n} t_i F(z_i) \tag{9}$$

where t_i are known weights.

3 APPLICATIONS

In this section, the workflow (Fig. 1) is used and results are demonstrated in two external and internal aerodynamic problems. In both, OpenFOAM was used for the evaluation of each aerodynamic shape.

3.1 Optimization of a 2D Isolated Airfoil Under Uncertainties

The first problem is dealing with the design of an airfoil (Fig. 3), in which the goal is to optimize its shape by maximizing the objective function $\hat{F} = \hat{\mu}_F - \hat{\sigma}_F$. The performance metric F is the lift coefficient C_L, $\hat{F}$ is thus defined in the worst case scenario. The initially generated CFD mesh has approximately 88K nodes and 160K elements. The flow conditions are: freestream Mach number $M_\infty = 0.15$ and Reynolds number based on the chord $Re_c = 3.33 \cdot 10^6$. The Spalart–Allmaras turbulence model [18] is used. The freestream flow angle (α_∞) is considered as the uncertain stochastic variable with mean value $\mu_{\alpha_\infty} = 5^o$ and standard deviation $\sigma_{\alpha_\infty} = 0.7^o$, which is assumed to follow a normal distribution. Before proceeding with the optimization, a UQ for the baseline geometry is carried out in order to decide about the PC order to be used. The results of this parametric study are tabulated in Table 1.

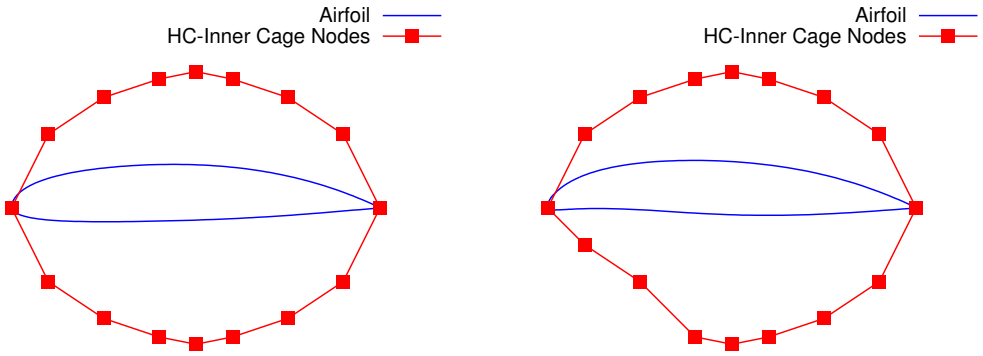

Figure 3: Shape optimization under flow uncertainties of an isolated airfoil parameterized using HC cages. Only the inner cage is shown, with just a small part of the flow domain; the CFD mesh is not drawn either. The coordinates of the control vertices of the red cage (red points), excluding those of the trailing and leading edge, stand for the design variables in this problem. Left: Initial geometry and HC inner cage with its control vertices. Right: Example of new HC inner cage position and the resulting airfoil shape.

Chaos Order q=1		Chaos Order q=2		Chaos Order q=3	
PCE - $\hat{\mu}_F$	0.879866	PCE - $\hat{\mu}_F$	0.880710	PCE - $\hat{\mu}_F$	0.879806
PCE - $\hat{\sigma}_F$	6.339144E-002	PCE - $\hat{\sigma}_F$	6.339217E-002	PCE - $\hat{\sigma}_F$	6.339199E-002

Table 1: Mean value and standard deviation of the lift coefficient of the starting/reference isolated airfoil. Computations performed using the non-intrusive PCE method.

From Table 1, it can been seen that chaos order $q = 2$ is a good compromise in terms of accuracy and computational cost (3 CFD evaluations are needed for the UQ of a single airfoil). The airfoil is parameterized using a pair of HC cages, as in Fig. 3. The inner/control cage comprises 16 nodes, 14 of which are allowed to vary in both directions summing up to 28 design variables in total. The leading and trailing edges are not allowed to move. A $(\mu, \lambda) = (8, 12)$ MAEA with μ parents and λ offspring was used for the optimization and the metamodels were activated after the first 30 evaluations. In the subsequent generations, all individuals were

pre–evaluated on the metamodels and the top two of them were selected for CFD–based re–evaluation. For a termination criterion of 200 evaluations an increase in the objective function ($\hat{F}$) by approximately 23% is achieved. In Fig. 4, the initial and the optimized geometry of the isolated airfoil are demonstrated along with the convergence of the optimization. The average cost per UQ on an Intel(R) Xeon(R) CPU E5-2630 v2 processor is 8 min. (on 6 cores), 88% of which stands for the cost of running the CFD evaluations.

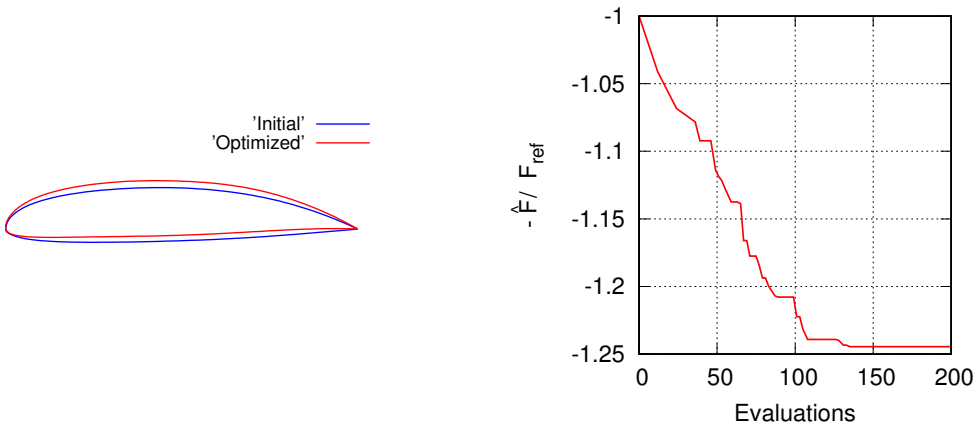

Figure 4: Initial and optimized shape of the airfoil is presented. Furthermore, the convergence history of the optimization is presented (for $-\hat{F}$).

3.2 Optimization of S-Bend Duct Under Uncertainties

The second case deals with the shape optimization of an S-bend duct for minimum $\hat{F} = \hat{\mu}_F + \hat{\sigma}_F$, with F being the total pressure losses across the duct. The latter is computed at the inlet/outlet cross sections, from the expression

$$\Delta p_t = \frac{\int (p + \frac{1}{2}\rho \vec{u}^2)\vec{u} \cdot \vec{n} dS}{\int \vec{u} \cdot \vec{n} dS} \tag{10}$$

where $\vec{u}$ is the velocity vector, p is the pressure and $\vec{n}$ is the unit outward normal vector at the boundaries of the flow domain.

The 3D CFD mesh has been generated using CFD-GEOM and consists of hexahedrals at walls, a zone of prisms and tetrahedra everywhere else. The flow is laminar with Re=550. As uncertain variables, the inlet velocity and the kinematic viscosity are used. It is assumed that both uncertain variables follow normal distributions with mean values and standard deviations as in Table 2.

Uncertain Variable	mean value	standard deviation
$U_{in}(m/s)$	10	0.5
$\nu(m^2/s)$	10^{-3}	$5 \cdot 10^{-5}$

Table 2: Mean values and standard deviations of the two uncertain variables in the S–bend duct optimization problem. Both follow normal distributions.

In Fig. 5, the initial shape of the duct is presented. The grey part of the geometry remains fixed whereas the (green) central curved part is free to deform.

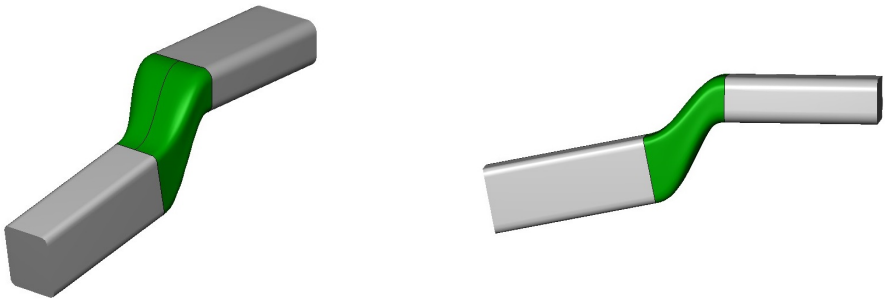

Figure 5: Initial shape of the S–bend duct problem. The grey part of the duct is fixed (undeformable) during the optimization whereas the green area is free to deform.

Initially, a UQ study has been performed so as to make a decision on the appropriate chaos order. From Table 3, it is concluded that using chaos order equal to q=2 (9 CFD evaluations per UQ) is acceptable in terms of computational cost in order to compute the statistical moments of F.

Chaos Order q=1		Chaos Order q=2		Chaos Order q=3	
PCE - $\hat{\mu}_F$	137.89217	PCE - $\hat{\mu}_F$	137.73546	PCE - $\hat{\mu}_F$	137.77606
PCE - $\hat{\sigma}_F$	11.14798	PCE - $\hat{\sigma}_F$	10.93479	PCE - $\hat{\sigma}_F$	11.08064

Table 3: Optimization of the S–bend duct. Mean value and standard deviation of total pressure losses for each of the user-defined chaos order.

After having decided the chaos order, the central curved part of the duct, which is free to deform, is parameterized using RBF. The coordinates of the 24 RBF centers are selected as design variables for the optimization workflow using EASY. For this case a $(\mu, \lambda) = (8, 12)$ MAEA was used for the optimization along with a termination criterion of 150 evaluations. Metamodels were activated after the first 25 evaluations and, in each subsequent generation, the three top individuals were selected for CFD–based re–evaluation. After the optimization in this duct, the objective function ($\hat{F}$) is reduced approximately by 10% and the changes in shape are shown in Fig. 6. The average cost per UQ on an Intel(R) Xeon(R) CPU E5-2630 v2 processor is 38 min., about 94% of which is the cost of performing the 9 CFD evaluations.

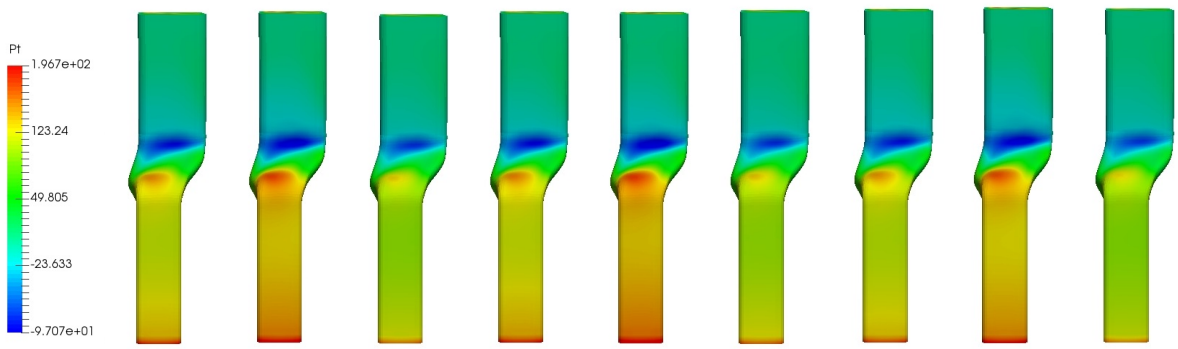

Figure 6: Optimization of the S–bend duct. Total pressure distribution in the optimal duct at each Gaussian node (i.e. set of flow conditions) indicated by the Gauss integration formula. This optimal duct yields about 10% less $\hat{F}$ value than the starting geometry.

4 CONCLUSIONS

This paper presents an automated workflow for performing aerodynamic shape optimization under flow uncertainties. The UQ of the performance metric is based on the non–intrusive PCE technique. CAD–free approaches (RBF or HC cages) are controlling the shape under consideration and R3M with its adaptive smoother are responsible for adapting the CFD mesh to the updated geometry. The shape optimization is performed by an Evolutionary Algorithm assisted by surrogate evaluation models. The new optimization platform has great potential and each and every of its components could readily be replaced by other tools with the same functionalities.

5 ACKNOWLEDGEMENTS

This work has been conducted within the IODA ITN on: "Industrial Optimal Design using Adjoint CFD". The first author is an Early Stage Researcher (ESR) in this project which has received funding from the European Union's Horizon 2020 Research and Innovation Programme under the Marie Sklodowska–Curie Grant Agreement No. 642959.

REFERENCES

[1] D. Xiu and G.E. Karniadakis. The Wiener - Askey polynomial chaos for stochastic diferrential equations. *SIAM Journal on Scientific Computing*, 24(2):619–644, 2002.

[2] The EASY (Evolutionary Algorithms SYstem) software, http://velos0.ltt.mech.ntua.gr/EASY., 2008.

[3] G.S. Eleftheriou and G. Pierrot. Rigid motion mesh morpher: A novel approach for mesh deformation. In *OPT-i, An International Conference on Engineering and Applied Sciences Optimization*, Kos, Greece, 4-6 June 2014.

[4] X. Lu and H. Li. Perturbation Theory Based Robust Design Under Model Uncertainty. *Journal of Mechanical Design*, 131(11), 2009.

[5] C. Hamarat, J. H. Kwakkel, and E. Pruyt. Adaptive Robust Design under deep uncertainty. *Technological Forecasting and Social Change*, 80(3):408–418, 2013.

[6] S. Asmussen and P. W. Glyn. *Stochastic Simulation: Algorithms and Analysis*. Stochastic Modelling and Applied Probability. Springer New York, 2007.

[7] W. Morokoff and R. Caflisch. Quasi-Monte Carlo integration. *Journal of Computational Physics*, 122(2):218–230, 1995.

[8] M.D. McKay. Latin Hypercube Sampling as a Tool in Uncertainty Analysis of Computer Models. In *Proceedings of the 24th Conference on Winter Simulation*, WSC '92, 557–564, New York, NY, USA, 1992. ACM.

[9] E.M. Papoutsis-Kiachagias, Papadimitriou D.I. and K.C. Giannakoglou. Robust design in aerodynamics using 3rd-order sensitivity analysis based on discrete adjoint. application to quasi-1d flows. *International Journal for Numerical Methods in Fluids*, 69(3):691–709, 2012.

[10] E.M. Papoutsis and K.C Giannakoglou. Continuous Adjoint Methods for Turbulent Flows, Applied to Shape and Topology Optimization. Industrial Applications. *Archives of Computational Methods in Engineering*, 23(2):255–299, 2016.

[11] D.I. Papadimitriou and K.C. Giannakoglou. Third-order sensitivity analysis for robust aerodynamic design using continuous adjoint. *International Journal for Numerical Methods in Fluids*, 71(5):652–670, 2013.

[12] M.S. Eldred and J. Burkardt. Comparison of Non-Intrusive Polynomial Chaos and Stochastic Collocation Methods for Uncertainty Quantification. *American Institute of Aeronautics and Astronautics*, 2009.

[13] CFD Research Corporation. *CFD-ACE Theory Manual, https://books.google.de/books?id=FinRGwAACAAJ.* CFD Research Corporation, 1993.

[14] M.K. Karakasis, A.P. Giotis and K.C. Giannakoglou. Inexact information aided, low-cost, distributed genetic algorithms for aerodynamic shape optimization. *International Journal for Numerical Methods in Fluids*, 43(10-11):1149–1166, 2003.

[15] M.K. Karakasis and K.C. Giannakoglou. On the use of metamodel-assisted, multi-objective evolutionary algorithms. *Engineering Optimization*, 38(8):941–957, 2006.

[16] P. Joshi, M. Meyer, T. DeRose, B. Green and T. Sanocki. Harmonic coordinates for character articulation. *ACM Trans. Graph.*, 26(3), July 2007.

[17] D.H. Kapsoulis, K.T. Tsiakas, V.G. Asouti and K.C. Giannakoglou. The use of kernel pca in evolutionary optimization for computationally demanding engineering applications. In *2016 IEEE Symposium Series on Computational Intelligence (IEEE SSCI 2016)*, Athens, Greece, December 6-9 2016.

[18] P.R. Spalart and S.R. Allmaras. A One-Equation Turbulence Transport Model for High-Reynolds Number Wall-Bounded Flows. *AIAA Paper 1992, 30th Aerospace Sciences Meeting and Exhibit*, January 6-9, 1992.